Bull. Mater. Sci. (2018) 41:79
https://doi.org/10.1007/s12034-018-1604-4

Physical, optical and structural studies of copper-doped lead oxychloro borate glasses

K CHANDRA SEKHAR[1,*], ABDUL HAMEED[1], VASANT G SATHE[2], M NARASIMHA CHARY[1] and MD SHAREEFUDDIN[1]

[1]Department of Physics, Osmania University, Hyderabad 500007, India
[2]UGC-DAE Consortium of Scientific Research, Khandwa Road, Indore 452017, India
*Author for correspondence (chandu_07u@yahoo.co.in)

MS received 10 July 2017; accepted 8 November 2017; published online 23 May 2018

Abstract. Bluish coloured glasses are obtained from the composition $PbCl_2$–PbO–B_2O_3 doped with Cu^{2+} ions. Basic physical properties and spectroscopic studies (optical absorption, electron paramagnetic resonance, Fourier transform infrared and Raman spectroscopies) were carried out on these samples. The increase in $PbCl_2$ content resulted in the decrease in density and increase in molar volume. At optical frequencies, band gaps and Urbach energies were evaluated and their variation is explained. Spin-Hamiltonian parameters (SHP) obtained from the EPR spectra suggest that the ligand environment around Cu^{2+} is tetragonally distorted octahedral sites and the orbital $d_{x^2-y^2}$ is the ground state. The characteristics broad bands in the optical absorption spectra are assigned to the $^2B_{1g} \rightarrow {}^2B_{2g}$ transition. The bonding coefficient values were evaluated using optical data and SHP. FTIR studies suggested that the glass structure is built up of BO_3 and BO_4 units. The presence of diborate, pyroborate, pentaborate groups, etc. in the glass network was confirmed from Raman spectra.

Keywords. Lead borate glasses; ionic radius; electro negativity; spin-Hamiltonian parameters; FTIR; Raman spectra.

1. Introduction

Due to the flexibility in the composition and with extremely interesting properties have made the glasses to attract many researchers. The importance of borate glasses increased in the last few decades, because they exhibit exclusive unique properties like durability, reduced thermal expansion, resistant to thermal shocks, enhanced toughness, chemical resistance, transparency, etc. Three-dimensional borate networks consist of BO_3 triangles and BO_4 tetrahedra. Glasses prepared with heavy metal oxide, such as PbO, CdO, BaO have shown relatively high index of refraction, density and transparency in IR radiation, etc. [1,2]. The addition of heavy metal oxides to the borate glass system increases the Raman scattering cross-section by several folds, thus, stimulating the interest in the complex systems [3]. Among the most metallic oxide glasses, lead oxide (PbO) glasses are unique. Even though the element lead is toxic, PbO plays an important role in the glass formation and has several advantages. PbO not only influences the structure, but also plays the dual role of modifier/former based on its concentration. At low concentration (<40 mol%), PbO behaves as network modifier in which Pb–O bond is ionic, while at higher concentration (>40 mol%), PbO acts as network former, where Pb–O bond is covalent [4–7]. Oxyhalide glasses are quite important for applications as host materials in high power laser systems. The inclusion of PbO and PbX_2 (X = F, Cl and Br) in the borate composition resulted in creating BO_3 and BO_4 units with the further considerable increase in transparency in IR radiation, high refractive index and optical nonlinearities. Lead glasses with halides have special optical properties leading to applications in modern optical devices, such as laser engineering and drawing of optical fibres [8–11]. Electron paramagnetic resonance (EPR) technique can present extensive knowledge about the microscopic local environment of the transition metal (TM) ions in glasses, which in turn are influenced by the local structure. The existence of TM ions in more than two valency states has attracted the attention of many researchers to dope the glasses with TM ions. Of the TM ions, copper has simple EPR spectrum and gives useful structural information about the ligands surrounding the Cu^{2+} ion in glass. Incorporation of paramagnetic ions such as Cu^{2+} enhances the applications of glasses towards memory and switching devices [12,13]. Keeping in view of the applications of halide glasses, the authors have investigated the physical, optical and structural studies of lead chloroborate glasses containing Cu^{2+}ions.

2. Experimental

Conventional melt-quenching method is used to prepare the glasses with $x$$PbCl_2$–$(30-x)$PbO–$69B_2O_3$–1CuO (PCPBC) (where x = 5, 10, 15, 20 and 25 mol%) composition. Analar

Table 1. Density (ρ), molar volume (V_m), optical band gap (E_{opt}, eV), refractive indices (n), molar refraction (R_m) and molar electronic polarizability (α_m) of xPbCl$_2$–(30 − x)PbO–69B$_2$O$_3$–1CuO (x = 5,10,15, 20 and 25 mol%) glasses.

Glass	Composition (mol%)				ρ (g cc^{-1})	V_m (cc mol^{-1})	ΔE (eV)	E_{opt} (eV)	n	R_m (cc mol^{-1})	α_m (10^{-24}) (cc mol^{-1})
	PbCl$_2$	PbO	B$_2$O$_3$	CuO							
PCPBC-1	5	25	69	1	4.358	35.75	0.670	2.46	2.50	22.84	9.04
PCPBC-2	10	20	69	1	4.180	37.93	0.267	2.69	2.47	22.69	8.98
PCPBC-3	15	15	69	1	4.025	40.07	0.285	2.80	2.44	24.70	9.78
PCPBC-4	20	10	69	1	3.882	42.26	0.347	3.06	2.39	24.50	9.70
PCPBC-5	25	5	69	1	3.754	44.43	0.295	3.20	2.35	31.72	12.56

grade chemicals, boric acid (H_3BO_3), lead chloride ($PbCl_2$), lead oxide (PbO) and cupric oxide (CuO) were taken as the initial starting materials. The glass mixture ratio for the present study is mentioned in table 1. Five grams of homogeneous batches were taken in porcelain crucible and sintered at 900°C for 45 min in an electrically heated furnace. The molten mixture was frequently stirred to get homogeneity and then, the melt was quenched. The obtained glasses were annealed at 200°C to remove thermal stress and strains. Thus formed glasses were bubble free, transparent and blue in colour and the thickness of the glass samples was ≈1 mm. X-ray diffractograms (XRD) of the glass samples were recorded at room temperature (RT). Density measurements are carried out using Archimedes principle. The uncertainty in the measurement of density is ±0.001. Polished glass samples were used for optical absorption measurements, which were carried out on Shimadzu UV-1800 series spectrometer at RT in the wavelength region of 200–1000 nm in absorbance mode. Electron paramagnetic resonance (EPR) spectra of the PCPBC glass series was recorded at RT using (BRUKER) EPR spectrometer operating at an X-band frequency (9.7 GHz) with a modulating frequency of 100 kHz. The magnetic field was scanned from 2500–4000G. The approximate error in the values of g and A were about ±0.002 and ±2 × 10^{-4}cm^{-1}, respectively. The Fourier transform infrared (FTIR) spectra of these samples are scanned in the range of 400–1600 cm^{-1} on Shimadzu 8400S FTIR spectrometer at RT. The micro Raman spectrum was recorded at RT using Jobin Yvon Horibra LABRAM-HR Raman spectrometer with Argon laser source of excitation wavelength of 488 nm.

3. Results and discussion

3.1 *XRD*

Figure 1 presents the XRD patterns of the prepared glasses. The spectrum of each glass system was examined, which revealed the absence of Bragg peaks, indicating the amorphous nature of the glasses. The broad hump also suggests the presence of short range order.

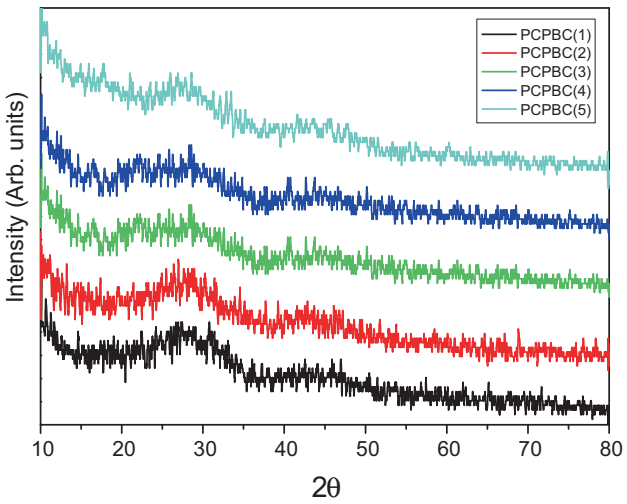

Figure 1. X-ray diffractograms of PCPBC glass system.

3.2 *Density and molar volume*

Density is the basic physical property, which explores the toughness and structural changes in any material. The variation of density depends on the coordination number, cross-link density, the size of interstitial positions and compactness [14]. Density (ρ_{exp}) measurements were carried out using Archimedes principle

$$\rho_{exp} = \frac{W_a}{W_a - W_b}\rho_b, \quad (1)$$

where W_a and W_b are the weights in air and xylene of the sample, respectively, and ρ_b the density of xylene (ρ_b = 0.865 g cc^{-1}). The molar volume (V_m) was estimated from the density and the molecular weight (M) of the glass samples. The response of ρ_{exp} and V_m with compositional parameter PbCl$_2$ is plotted in figure 2. It was found that the density decreases with increasing PbCl$_2$ concentration, and molar volume showing exactly opposite behaviour. This variation is because of the ionic radius of chlorine (1.81 Å) is greater than oxygen (1.4 Å) and Cl$^-$ ion may occupy more space and spans

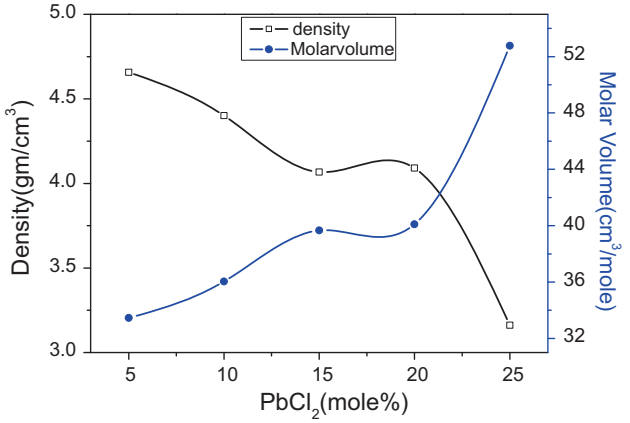

Figure 2. Variations of density and molar volume with $PbCl_2$ content.

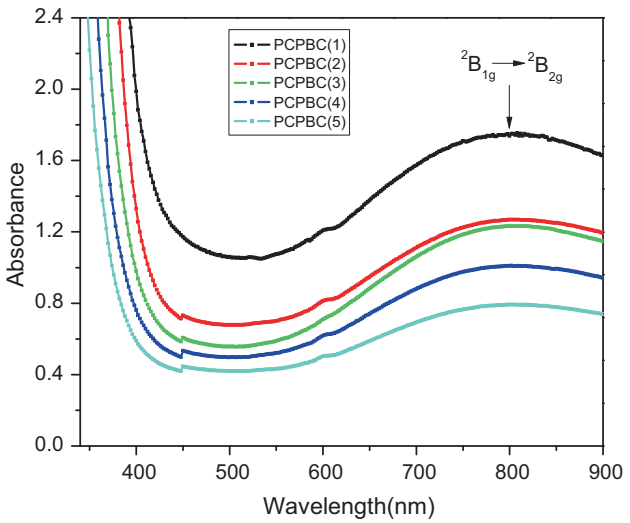

Figure 3. Optical absorption spectra of PCPBC glass system.

the glass network, thereby increasing molar volume. To accommodate the large Cl^- ions, the glass network forms an open structure and the Cl^- ions are located in the interstices [15,16].

3.3 *Optical absorption spectra*

Figure 3 shows the spectra of optical absorption of all the glass compositions xPbCl$_2$–(30 − x)PbO–69B$_2$O$_3$–1CuO. The broad absorption band in the spectra is assigned to $^2B_{2g} \rightarrow {}^2B_{1g}$ transition. No sharp absorption edges are found in the spectra, which further confirm the glassy nature. The absorption coefficient, $\alpha(\upsilon)$ is obtained for different photon energies using the relation;

$$\alpha(\upsilon) = 2.303\frac{A}{d}, \tag{2}$$

where A is the absorbance and d is the thickness of the sample.

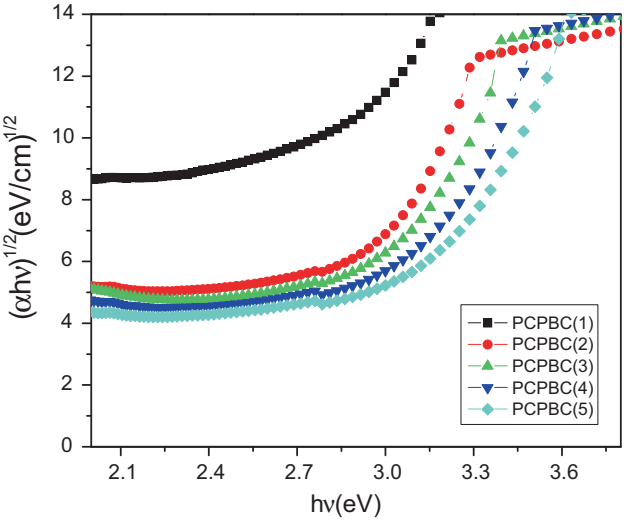

Figure 4. Tauc's plot of PCPBC glass system.

3.4 *Optical band gap and Urbach energy*

Figure 4 shows the Tauc's plot of prepared samples. The UV absorption edge is shifted to lower wavelength (i.e., blue-shifted) side with increase in $PbCl_2$ content. According to Davis and Mott, optical band gap and photon energy are related as [17]:

$$(\alpha h\upsilon) = B^2\left(h\upsilon - E_g\right)^r. \tag{3}$$

Physical quantities in the above equation have their usual meanings. Optical band gaps are obtained by extrapolating the linear region of the indirect allowed transition curve to $(\alpha h\upsilon)^{1/2} = 0$. In the present study, optical band gap values are increasing with increase in $PbCl_2$. The electro negativity of chlorine ion (3.16) is relatively smaller when compared with the electronegativity of oxygen ion (3.44). When $PbCl_2$ content is increasing, the ionicity of oxygen ions decreases, and hence optical band gap increases [15,18,19].

Urbach rule states that the absorption coefficient increases exponentially with photon energy [20–22]. Urbach's expression is given by

$$\alpha(\nu) = C\exp\left(h\nu/\Delta E\right), \tag{4}$$

where C is a constant and ΔE the Urbach energy.

Urbach energy (ΔE) values were obtained by taking the inverse slopes of the straight line portion of the graph drawn between ln(α) and $h\upsilon$. The nonlinear variation of Urbach energy (ΔE) with $PbCl_2$ concentration is shown in figure 5. This nonlinear variation might be due to nonuniform distribution of defects in the glass matrix with increase of $PbCl_2$.

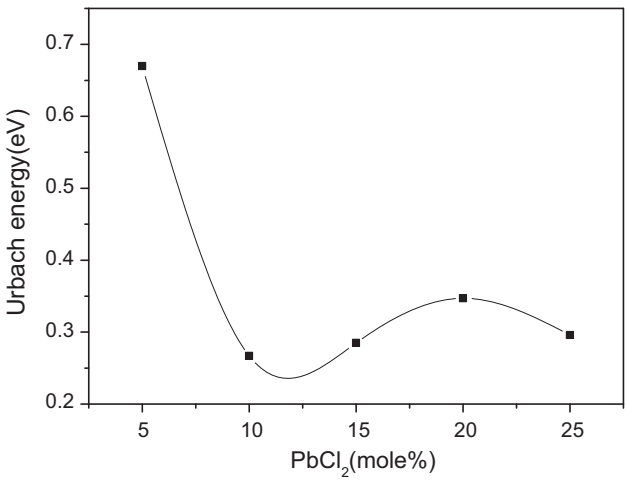

Figure 5. Variation of Urbach energy (ΔE) with $PbCl_2$ content.

3.5 *Refractive index, molar refraction and molar electronic polarizability*

Dimitrova, Komatshu and Duffy [23–25] proposed a relation to evaluate the refractive index, molar refraction and molar polarizibility of the glasses, which are given below:

$$\frac{n^2-1}{n^2+2} = 1 - \sqrt{\frac{E_{\text{opt}}}{20}}, \tag{5}$$

$$R_{\text{M}} = \frac{n^2-1}{n^2+2} * V_{\text{m}}, \tag{6}$$

$$\alpha_{\text{m}} = \left(\frac{3}{4\Pi N_{\text{A}}}\right) * R_{\text{m}}. \tag{7}$$

where n is the refractive index, V_{m} the molar volume, the term $(n^2-1)/(n^2+2)$ represents the reflection loss and N_{A} the Avogadro's number. The n values are in the range 2.73–2.35. From equation (5), it is clear that the refractive index values are decreasing with the increase in optical band gap, while from equations (6) and (7), molar refraction and electronic polarizability are proportionally increasing with molar volume. The evaluated values of refractive index, molar refraction and electronic polarizability of these glasses are given in table 1.

3.6 *EPR spectra*

A neutral copper atom with atomic number $Z = 29$ has an electronic configuration [Ar] $3d^{10}\ 4s^1$. Copper atom acquires [Ar] $3d^9$ configuration in its +2 oxidation state by losing one electron from 3d and 4s each and becomes Cu^{2+} ion. The effective spin of Cu^{2+} ion is $S = 1/2$ and the nuclear spin (I) is 3/2. Hyperfine structure observed in the EPR spectrum is due to the interactions between the nuclear and electronic magnetic moments both in spin and orbital. Each fine structure line is expected to split into four hyperfine lines in accord with

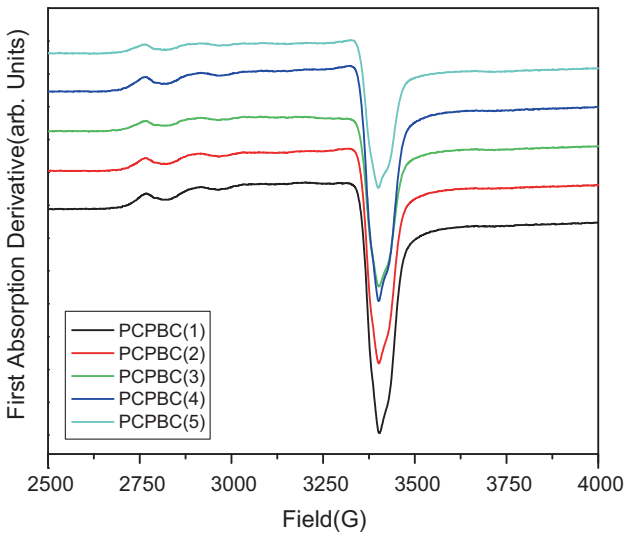

Figure 6. Electron paramagnetic resonance spectra of PCPBC glass system.

$2I + 1$. Figure 6 shows the EPR spectra of $x PbCl_2$–$(30 - x)$ PbO–$69B_2O_3$–1CuO glass system. In the present work, three weak parallel hyperfine splittings were observed in the range of 2750–3000G, while the fourth line merged with the perpendicular components. The analysis of EPR spectra is done using the spin-Hamiltonian [26].

$$\mathcal{H} = \beta\left[g_{\parallel} H_{\text{Z}} S_{\text{Z}} + g_{\perp}\left(H_{\text{X}} S_{\text{X}} + H_{\text{Y}} S_{\text{Y}}\right)\right] + A_{\parallel} I_{\text{Z}} S_{\text{Z}} + A_{\perp}\left(I_{\text{X}} S_{\text{X}} + I_{\text{Y}} S_{\text{Y}}\right), \tag{8}$$

where Z is the symmetry axes of copper centres and other symbols have usual notations. The nuclear quadrapole interaction is so small to be considered in the analysis of the spectra. The expression for g and A tensors for parallel and perpendicular peaks are obtained from the solution of the spin-Hamiltonian [27], as

$$h\nu = g_{\parallel}\beta H + mA_{\parallel} + \left(\frac{15}{4} - m^2\right)\frac{A_{\perp}^2}{2g_{\parallel}\beta H}, \tag{9}$$

$$h\nu = g_{\perp}\beta H + mA_{\perp} + \left(\frac{15}{4} - m^2\right)\frac{A_{\parallel}^2 + A_{\perp}^2}{4g_{\parallel}\beta H}. \tag{10}$$

The spin-Hamiltonian parameters are given in table 2. The observed g and A values and shape of the EPR spectra suggest that the CuO in all the glasses is existing as Cu^{2+} ion with $3d^9$ configurations. In the present work, it is noticed that $g_{\parallel}$ values are varied from 2.338 (PCPBC1) to 2.464 (PCPBC5), a significant variation in $g_{\parallel}$ values is observed. This might be due to the variation of ligand field strength around Cu^{2+} ion. $g_{\perp}$values varied between 2.064 (PCPBC1) and 2.066 (PCPBC5) and are almost constant. $g_{\parallel} > g_{\perp} > g_e$ ($g_e = 2.0023$) and $A_{|} > A_{\perp}$ suggest that the environment

Table 2. Spin-Hamiltonian parameters, number of spins, susceptibility and bonding parameters of xPbCl$_2$–(30 − x)PbO–69B$_2$O$_3$–1CuO (where x = 5, 10, 15, 20 and 25 mol%) glasses.

Glass	$g_\parallel$	$g_\perp$	$A_\parallel$ (10^{-4} cm^{-1})	$A_\perp$ (10^{-4} cm^{-1})	ΔE_{xy} (cm^{-1})	α^2	β^2	β_1^2	N (10^{21}) per kg	χ (10^{-4}) (m^3 kg^{-1})
PCPBC-1	2.338	2.064	151	34	12873	0.825	0.717	0.789	2.61	4.73
PCPBC-2	2.352	2.064	139	35	12801	0.805	0.735	0.833	2.99	5.43
PCPBC-3	2.355	2.066	139	39	12252	0.805	0.735	0.797	3.11	5.67
PCPBC-4	2.343	2.065	148	37	12478	0.819	0.722	0.775	2.66	4.83
PCPBC-5	2.464	2.066	148	39	12331	0.944	0.627	0.910	3.07	5.78

around Cu^{2+} ion is distorted octahedral (D_{4h}) site elongated along z-axis [28]. The variation of $g_\parallel$ and $A_\parallel$ with $PbCl_2$ content was found to be nonlinear, which suggest that there is a change in the tetragonal distortion around Cu^{2+} ion. For all the glass samples in the optical absorption spectra, a single asymmetric broadband near IR region was observed, which is shown in figure 3. This band can be identified as the d–d transition band due to Cu^{2+} ions and it is assigned to $^2B_{1g} \rightarrow {}^2B_{2g}$ transition (ΔE_{xy}). Bonding between the orbitals of Cu^{2+} ion with its ligands are described by α^2, β^2, and β_1^2. α^2 denote the in-plane σ-bonding of the ligand with $d_{x^2-y^2}$ orbital, the out-of-plane and in-plane Π-bonding of ligands (β^2 and β_1^2) with the d_{xz}, d_{yz} and d_{xy} orbitals, respectively [29,30]. The bonding parameters are given in table 2. The value of α^2 indicates ionic nature of the σ-bond, while β^2 and β_1^2 indicate moderately ionic nature of the in-plane and out-of-plane π-bonds.

The number of unpaired spins (N) of Cu^{2+} ions that are taking part in resonance can be estimated by comparing the area under the EPR spectra with that of standard spectra of $CuSO_4{\cdot}5H_2O$ compound as given by Weil *et al* [31].

Using N and g values, we estimated the paramagnetic susceptibility of each glass sample by using the relation [32].

$$\chi = \frac{Ng^2\beta^2 J\,(J+1)}{3k_B T}, \tag{11}$$

where J = 5/2, and the other symbols in the expression have their usual notations. The N and χ values are given in table 2. Even though, the transition metal (Cu) is fixed to 1 mol%, the number of spins participating in the resonance (N) is varying nonlinearly with the compositional parameter $PbCl_2$. It is understood that glass network plays a prominent role on N.

3.7 *FTIR*

Structural and functional groups in amorphous solids are identified by FTIR and Raman studies [33–35]. FTIR spectra of xPbCl$_2$–(30 − x)PbO–69B$_2$O$_3$–1CuO (where x = 5, 10, 15, 20 and 25 mol%) glasses are shown in figure 7. The observed band positions and assignments of FTIR spectra are listed in table 3. The wavenumbers <600 cm^{-1}(lower wavenumber side) are assigned to metallic cation vibrations in glasses

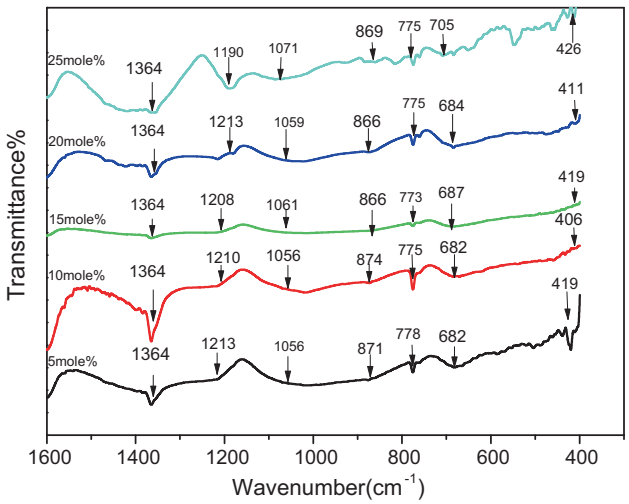

Figure 7. FTIR spectra of PCPBC glass system.

[35]. The observed band near 419 cm^{-1} is attributed to Pb^{2+} vibrations. Absorption bands observed in the range of 682–705 cm^{-1} are due to B–O–B bond-bending vibrations from the pentaborate group or may be due to bending vibrations of BO_3triangles [6]. The band observed near 775 cm^{-1} is due to O_3B–O–BO_4 bond-bending vibrations and at 870 cm^{-1} due to B–O stretching vibrations in BO_4 units from diborate rings [34]. A band near 1061 cm^{-1} is due to B–Ø stretching vibrations in $Ø_4^-$ unit from tri-, tetra- and penta-borate groups. The bands that arise due to stretching vibrations of trigonal BO_3 units from pyro- and ortho-borate groups are found near 1208 cm^{-1} and the presence of pyroborate and orthoborate groups containing BO_3^- are found at 1364 cm^{-1} [33,35].

3.8 *Raman spectra*

Raman spectra of the glass samples are shown in figure 8 and corresponding deconvoluted spectrum of PCPBC3 is shown in figure 9. Raman spectra are spread over in the region of 400–1600 cm^{-1}. The Raman spectra have shown bands at ∼691, ∼766, ∼796, ∼870, ∼955, ∼1051, ∼1114, ∼1246, ∼1335, ∼1415 and ∼1502 cm^{-1}(table 3). The band at ∼691 cm^{-1}

Table 3. Assignment of FTIR and Raman bands in the spectra of xPbCl$_2$–(30 − x) PbO–69B$_2$O$_3$–1CuO glass system.

FTIR		Raman	
Wavenumber (cm^{-1})	Assignment	Wavenumber (cm^{-1})	Assignment
~419	Pb^{2+} vibrations	~691	Existence of $BO_2O_2^{3-}$ unit
~687	B–O–B bond-bending vibrations from pentaborate group or bending vibrations of BO_3traingles	~766	Symmetric breathing vibrations of six-member rings with one or two $BØ_3$ triangles replaced by $BØ_4^-$tetrahedra.
~775	O_3B–O–BO_4 bond-bending vibrations	~796	Symmetric breathing vibrations of boroxol rings.
~866	B–O stretching vibrations in BO_4 units from diborate rings	~870	Symmetric stretching vibrations of B–O–B bridges in pyroborate units.
~1061	B–O stretching vibrations in BO_4 units from tri-, tetra- and penta-borate groups	~955	Due to pentaborate and tetraborate groups
~1208	Stretching vibrations of tetragonal BO_3 units from pyroborate and orthoborate groups	~1051	Attributed to presence of diborate groups
~1364	Presence of pyroborate and orthoborate groups containing BO_3^-	~1114	Diborate groups
		~1246	Pyroborate groups
		~1335	$BØ_2O^-$ triangles linked to $BØ_4^-$units
		~1415	Stretching of B–O bands attached to large number of borate groups
		~1502	$BØ_2O^-$ triangles linked to other borate triangular units

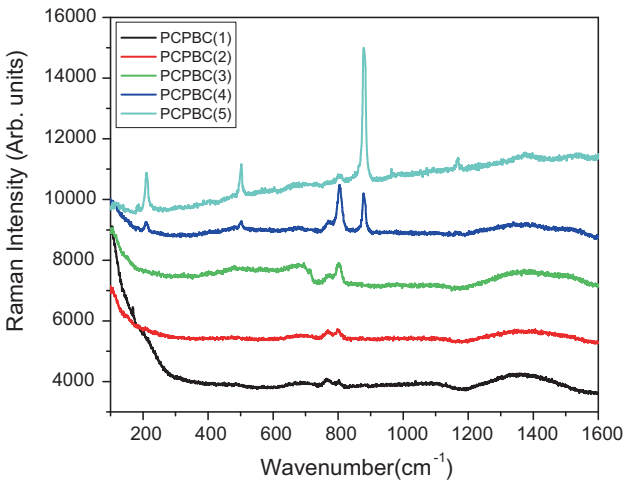

Figure 8. Raman spectra of PCPBC glass system.

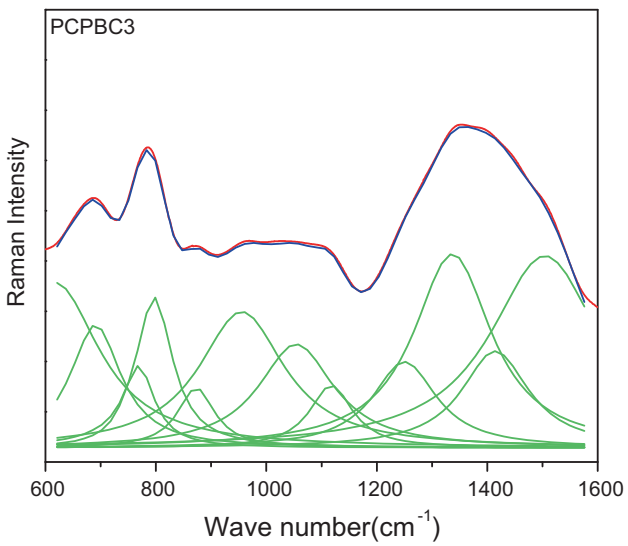

Figure 9. Deconvoluted Raman spectra of PCPBC3 glass.

shows the existence of $BO_2O_2^{3-}$ unit [38]. The band centred at ~766 cm^{-1} can be assigned to symmetric breathing vibrations of six-member rings with one or two $BØ_3$ triangles replaced by $BØ_4^-$tetrahedra. The band at ~796 cm^{-1} is assigned to symmetric breathing vibrations of boroxol rings, it is shifting towards higher wavenumber side (i.e., 796–806 cm^{-1}) and its intensity is increasing with the increase of $PbCl_2$ content. The band at ~870 cm^{-1} is due to symmetric stretching vibrations of B–O–B bridges in pyroborate units and it is shifted to 880 cm^{-1} with increasing intensity for 20 and 25 mol% of $PbCl_2$ [34,38]. As $PbCl_2$ content is increasing, the peak intensity of 796 cm^{-1} is increasing, which might be due to the formation of pentaborate groups [39]. For 20 and 25 mol% of $PbCl_2$, a new band at 500 cm^{-1} appeared, which is also confirming the

formation of pentaborate group. The band at ∼955 cm^{-1} is due to pentaborate and tetraborate groups. The band around ∼1051 cm^{-1} is attributed to the presence of diborate groups. The bands at ∼1114 and ∼1246 cm^{-1} are due to diborate and pyroborate groups, respectively. The band at ∼1335 cm^{-1} is due to $B\emptyset_2O^-$ triangles linked to $B\emptyset_4^-$ units. The band at ∼1415 cm^{-1} is assigned to stretching of B–O bands attached to the large number of borate groups and at ∼1502 cm^{-1} due to $B\emptyset_2O^-$ triangles linked to other borate triangular units [34–41].

4. Conclusions

$x$$PbCl_2$–$(30 - x)$PbO–$69B_2O_3$–1CuO (where x = 5, 10, 15, 20 and 25 mol%) glasses were prepared by the melt quenching method. From XRD spectra, the amorphous nature of the glasses was confirmed. Molar volume is increasing, while the density is decreasing with the increase of $PbCl_2$ since ionic radius of chlorine ion is greater than oxygen. A broad absorption band is observed in the optical absorption spectra, which were assigned to $^2B_{1g} \rightarrow {}^2B_{2g}$ transition. Optical band gap values are increasing with $PbCl_2$ content, which is due to the decrease in iconicity of oxygen ions with $PbCl_2$ content. From the EPR spectra, it was concluded that the ground state of Cu^{2+} ion is $d_{x^2-y^2}$ orbital ($^2B_{1g}$ state), the Cu^{2+} ions were located in tetragonally distorted octahedral sites. FTIR spectra of all the glasses showed bands in the mid-infrared region of 400–1600 cm^{-1}. The observed bands are assigned and some of the bands are attributed to B–O–B bond bending vibrations and stretching vibrations of BO_3, BO_4 units from various borate groups. Raman spectra of all the glasses exhibited bands in the region of 400–1600 cm^{-1}. These bands are attributed to the presence of diborate and pyroborate groups and some of these bands exhibit symmetric breathing vibrations of six-membered rings and boroxol rings.

References

[1] Dahiya M S, Khasa S and Agarwal A 2015 *J. Asian Ceram. Soc.* **3** 206

[2] Upender G, Ramesh S, Prasad M, Sathe V G and Mouli V C 2010 *J. Alloys Compd.* **504** 468

[3] Ignatieva L N, Savchenko N N, Yu Marchenko V, Maslennikova I G and Zverev G A Goncharuk 2016 *J. Non-Cryst. Solids* **450** 103

[4] Rao K J, Rao B G and Elliott S R 1985 *J. Mater. Sci.* **20** 1678

[5] Laxmikanth C, Raghavaiah B V, Appa Rao B and Veeraiah N 2004 *J. Lumin.* **109** 193

[6] Saddeek Yasser B 2017 *Bull. Mater. Sci.* **40** 545

[7] Saddeek Yasser B 2009 *J. Alloys Compd.* **467** 14

[8] Yousef E S S 2007 *J. Mater. Sci.* **42** 4502

[9] Pisarska J, Zur L and Wojciech W A 2012 *Phys. Status Solidi A* **209** 1134

[10] Ghoneim N A, El Batal H A, Abdelghany A M and Ali I S 2011 *J. Alloys Compd.* **509** 6913

[11] Pisarski W A, Pisarska J, Lisiecki R, Grobelny Ł, Dominiak-Dzik G and Ryba-Romanowski W 2009 *Chem. Phys. Lett.* **472** 217

[12] Shareefuddin Md, Jamal Md and Narasimha Chary M 1995 *Phys. Status Solidi A* **148** K37

[13] Thulasiramudu A and Buddhudu S 2006 *J. Quant. Spectrosc. Radiat. Transf.* **97** 181

[14] Saddeek Yasser B, Aly K A and Bashier S A 2010 *Physica B* **405** 2407

[15] Chandra Sekhar K, Hameed A, Ramadevudu G, Narasimha Chary M and Shareefuddin Md 2017 *Mod. Phys. Lett. B* **31** 1750180

[16] El Damravi G 1994 *J. Non-Cryst. Solids* **176** 91

[17] Davis A and Mott N F 1970 *Philos. Mag*. **22** 903

[18] John Duffy A 2001 *Phys. Chem. Glasses* **42** 151

[19] Sebastian Shajo and Abdul Khadar M 2004 *Bull. Mater. Sci*. **27** 207

[20] Tauc J, Grigorovice R and Vancu A 1966 *Phys. Status Solidi* **15** 627

[21] Talib Z A, Daud W M, Tarmizi E Z M, Sidek H A A and Yunus W M M 2008 *J. Phys. Chem. Solids* **69** 1969

[22] Urbach F 1953 *Phys. Rev*. **92** 1324

[23] Dimitrov V and Sakka S 1996 *J. Appl. Phys*. **79** 1736

[24] Dimitrov V and Komatshu T 2002 *J. Solid State Chem.* **163** 100

[25] Duffy J A 1986 *J. Solid State Chem.* **62** 145

[26] Kivelson D and Neiman R 1961 *J. Chem. Phys.* **35** 149

[27] Bleaney B, Bowers K D and Pryce M H L 1955 *Proc. R Soc. A* **228** 147

[28] Thirumala Rao G, Babu B, Joyce Stella R, Pushpa Manjari V and Ravikumar R V S S N 2015 *Spectra Acta Part A* **139** 86

[29] Sands R H 1955 *Phys. Rev.* **99** 1222

[30] Shareefuddin Md, Jamal Mohd and Narasimha Chary M 1996 *J. Non-Cryst. Solids* **201** 95

[31] Weil J A, Bolton J R and Wertz J E 1994 *Electron paramagnetic resonance elementary theory and practical applications* (New York: Wiley) p 498

[32] Aschcroft N W and Mermin N D 2001 *Solid State Physics* (New York: Harcourt College Publishers) p 656

[33] Doweidar H and Saddeek Yasser B 2009 *J. Non-Cryst. Solids* **355** 348

[34] Ciceo-Lucacel R and Ardelean I 2007 *J. Non-Cryst. Solids* **353** 2020

[35] Sumalatha B, Omkaram I, Rajavardhana Rao T and Linga Raju Ch 2013 *Physica B* **411** 99

[36] Saddeek Y B 2009 *Philos. Mag.* **89** 41

[37] Dwivedi B P and Khanna B N 1995 *J. Phys. Chem. Solids* **56** 36

[38] Meera B N and Ramakrishna J 1993 *J. Non-Cryst. Solids* **159** 1

[39] Meera B N, Sood A K, Chandrabhas N and Ramakrishna J 1990 *J. Non-Cryst. Solids* **126** 224

[40] Padmaja G and Kistaiah P 2009 *J. Phys. Chem. A* **113** 2397

[41] Naresh V and Buddhudu S 2012 *Ceram. Inter.* **38** 2325